PROCEEDINGS OF SCIENCE

The impact of a modified CMB photon density on UHECR propagation

Janning Meinert,[a,b,*] **Leonel Morejon,**[a] **Alexander Sandrock,**[a] **Björn Eichmann,**[c] **Jonas Kreidelmeyer**[d] **and Karl-Heinz Kampert**[a]

[a] *Bergische Universität Wuppertal, Department of Physics, Gaußstraße 20, 42103 Wuppertal, Germany*
[b] *Institut für Theoretische Physik, Universität Heidelberg, Philosophenweg 12, 69120 Heidelberg, Germany*
[c] *Ruhr-Universität Bochum, Theoretische Physik IV, Fakultät für Physik und Astronomie, Universitätsstraße 150, 44801 Bochum, Germany*
[d] *Institut für Experimentalphysik, Universität Hamburg, DESY, Luruper Chaussee 149, Hamburg, Germany*
E-mail: meinert@uni-wuppertal.de, leonel.morejon@uni-wuppertal.de, asandrock@uni-wuppertal.de, eiche@tp4.rub.de, jonas.kreidelmeyer@desy.de, kampert@uni-wuppertal.de

The existing discrepancies between the observation of local and extraction of global cosmological parameters motivate an extension of the ΛCDM cosmological model. A proposed extension called $\mathrm{SU(2)_{CMB}}$ describes cosmic microwave background (CMB) photons with an SU(2) instead of a U(1) gauge group. This mitigates some of these tensions, for example H_0, Ω_m, σ_8, pushes the recombination epoch to higher redshifts, and thereby effectively reduces CMB photon densities. In this work, we study the impact of the SU(2) modified CMB evolution to the propagation of ultra-high energy cosmic rays (UHECRs) and their related fluxes of cosmogenic photons and neutrinos. The measured and predicted fluxes are the basis used to constrain source properties and rely on the ΛCDM CMB evolution. Thus, a modification of the past CMB densities impacts these flux predictions and possibly the constraints on the sources. In particular, we show an increased proton flux below the ankle ($10^{18.5}$ eV), and slightly increased cosmogenic neutrino fluxes in comparison to ΛCDM.

38th International Cosmic Ray Conference (ICRC2023)
26 July - 3 August, 2023
Nagoya, Japan

*Speaker

1. Introduction

The cosmic microwave background (CMB) stands as the foundation of contemporary Cosmology. Among its characteristics, there is an intriguing anomaly observed in the CMB line temperature at low frequencies, starting at around 1 GHz [9, 10, 21]. While radio sources originating from within our galaxy offer a plausible explanation, they fail to account for the isotropic nature of the excess radiation [21, 23]. Another potential contributor to this foreground signal could be the decay of axions with a mass of approximately 30 μeV (8 GHz), compare [8] for a general discussion of axion decays at radio frequencies. Alternatively, the excess in CMB line temperature can also be interpreted as an inherent characteristic of the CMB itself, rather than a result of foreground radio emissions [16]. We will pursue the latter explanation in this work.

Associating CMB photons with a thermal SU(2) gauge theory, the so-called $\mathrm{SU(2)_{CMB}}$, instead of a trivial thermal U(1) theory, introduces two interesting phase boundaries [17]. The CMB occurs in the deconfining phase, where the SU(2) gauge symmetry is broken down to U(1) due to densely packed topological field configurations, Harrington-Shepard anti-calorons and calorons [14]. For lower temperatures, in the so-called preconfining phase, U(1) is further reduced to the magnetic center group Z_2, which undergoes its own breaking within the confining phase. The transition from the deconfining to the preconfining phase occurs at a critical temperature T_c, which can be identified to be close to the current temperature of the CMB [16]. Spontaneously breaking the U(1) gauge group in the preconfined phase then leads to a Meissner mass of the photon of around 10 peV (100 MHz), compare [16]. This alternative explanation for the radiation excess as an intrinsic feature of the cosmic microwave background demands adjustments to the current cosmological model ΛCDM.

One notable change is observed in the temperature-redshift relation $T(z)$ of the CMB photons. Within flat ΛCDM and in adiabatically evolving cosmological models, the $T(z)$-relation is $T(z)/T_0 = (1+z)$, where $T_0 = 2.725\,\mathrm{K}$ is the present CMB temperature [19]. Implementing an SU(2) gauge group into ΛCDM leads to $T(z)/T_0 = 1/4^{1/3}\,(1+z)$ for large redshifts $z \gg 1$, see also [11]. This means that the CMB photons are cooling down slower with the expansion of the Universe in $\mathrm{SU(2)_{CMB}}$ than in ΛCDM. The changed $T(z)$ thus requires recombination to occur at a higher redshift. When the CMB multipoles are fitted with the changed $T(z)$, recombination occurs at $z_{*,\mathrm{SU(2)}} = 1715 \pm 0.19$ [13] and is thereby at significantly higher redshift than in normal ΛCDM with $z_{*,\mathrm{U(1)}} = 1089.92 \pm 0.25$ [5].

The relatively high recombination redshift has mainly two consequences: Firstly, the CMB fit does not work, unless more matter is introduced to the cosmological model at some point after recombination [13]. Secondly, the consequence of this high recombination redshift is stretching the CMB photon density over longer periods of time, and thus increases the interaction lengths for ultra-high energy cosmic rays.

While there exist many attempts of measuring the $T(z)$ indirectly, for example with absorber clouds [20], it is not obvious that those indirect methods are sensitive to the actual CMB temperatures at finite redshifts [18]. They might only probe the temperature of the absorber clouds and the

blackbody nature of the CMB. Thus, there is a need to determine the temperature redshift relation of the CMB directly.

The consequences for UHECR interactions with an $SU(2)_{CMB}$ description have been discussed previously, only considering the handedness of the photons, $SU(2)_L$ [22]. A fully consistent understanding of the $SU(2)_{CMB}$ model requires applying Yang-Mills thermodynamics and obtaining the modified $T(z)$. Furthermore, the effect of this modified temperature redshift relation on the CMB density produces non-trivial redshift dependences on the UHECRs interactions that need to be considered in depth. The purpose of this work is to discuss the multi-messenger implications of employing the $SU(2)_{CMB}$ modified temperature redshift relation consistently.

Firstly, the modified $T(z)$ relation is outlined in section 2. The consequences of this relation for all the interactions of UHECRs are discussed in section 3. In section 4 we simulate UHECR propagation employing the best fit values of [15] to spectrum and composition data by the Pierre Auger Observatory. This is the basis for our comparison of different fluxes with U(1) and SU(2) $T(z)$ relations. We also show the corresponding cosmogenic neutrino fluxes for those fit parameters.

2. $T(z)$ relation of $SU(2)_{CMB}$

In the following, a brief review is given on how the $T(z)$ relation of deconfining $SU(2)_{CMB}$ thermodynamics is altered. For a longer version of the argument, the reader is referred to [12, 18]. The $T(z)$ relation is generally given by

$$T(z) = \mathcal{S}(z)(z+1)\,T_0\,, \tag{1}$$

where $\mathcal{S}(z)$ is a scaling factor which is $\mathcal{S}(z)_{U(1)} = 1$ for ΛCDM. The core idea for SU(2) dominated CMB radiation is that the additional degrees of freedom in an SU(2) gauge group lead to the topological constant $1/4^{1/3}$ at large $z \gg 1$, so that

$$T(z)/T_0 = \left(\frac{1}{4}\right)^{1/3}(1+z)\,, \qquad (z \gg 0). \tag{2}$$

For smaller redshifts, this linear modification of $T(z)$ does not work and the nonlinear function $\mathcal{S}(z)_{SU(2)}$ as derived in [13] has to be used. This function $\mathcal{S}(z)_{SU(2)}$ can be approximated reasonably well with the analytical function for low z

$$\mathcal{S}(z)_{SU(2)} \approx \exp(1 - 1.7\,z) + \left(\frac{1}{4}\right)^{1/3}, \qquad (z \lesssim 4). \tag{3}$$

This approximation will be used in section 3. However, the numerical solution will be applied in section 4.

3. Changes in propagation length

In this section, we briefly discuss the differences of propagating ultra-high energy cosmic rays under a normal and modified $T(z)$-relation as mentioned in the previous section, Eqs. 2 and Eqs. 3. The redshift dependence of the CMB temperature results in scaling and shifting of the differential CMB photon number density $n_{\mathrm{CMB}}(\epsilon, z)$ which is given by

$$n_{\mathrm{CMB}}(\epsilon, z) = \left(\frac{T(z)}{T_0}\right)^2 n_{\mathrm{CMB}}\left(\epsilon\left(\frac{T(z)}{T_0}\right)^{-1}, 0\right), \tag{4}$$

where ϵ is the energy of the photons and n_{CMB} is given by the Planck distribution as

$$n_{\mathrm{CMB}}(\epsilon, z) = \frac{8\pi}{(hc)^3}\frac{\epsilon^2}{\exp(\epsilon/k_B T(z)) - 1}. \tag{5}$$

The redshift dependence of UHECR interactions with the CMB is reflected in the expression for the energy loss length [7]

$$-\frac{1}{E}\frac{dE}{dx} = kT(z)\int_{\epsilon_0}^{\infty}\frac{d\epsilon'(\epsilon')\sigma(\epsilon')f(\epsilon')}{2\pi^2\gamma^2(c\hbar)^3}\left\{-\ln\left[1-\exp\left(-\frac{\epsilon'}{2\gamma kT(z)}\right)\right]\right\} \tag{6}$$

where E is the energy of the UHECRs and $\sigma(\epsilon')$ is the cross-section for the corresponding interaction (photodisintegration, photomeson, pair-production) and $f(\epsilon')$ is the average inelasticity of the interaction. The scaling of the CMB density is reflected in a scaling of the interaction rates

$$\lambda(\gamma, z)^{-1} = \left(\frac{T_0}{T(z)}\right)^3 \lambda^{-1}\left(\frac{T(z)}{T_0}\gamma, z = 0\right) \tag{7}$$

The comparison of the energy loss lengths for U(1) and SU(2) is shown in Fig. 1 a) (protons) and in Fig. 1 b) (silicon) for $z = 1$. The interaction processes with the CMB are represented separately (photopion, photodisintegration, pair production) while they are grouped into one curve for extra-galactic background light (EBL, dotted dark red). For the protons at redshift $z = 1$, SU(2) shifts the threshold and increases the propagation length by a factor of ~ 3 for energies above 10^{11} GeV. For silicon nuclei at the same redshift, the thresholds are also shifted to higher energies, however, the difference of the two CMB photon densities below 10^{11} GeV is overshadowed by the interactions of the UHECRs with the EBL. This is why proton abundance below the ankle is pronounced, but heavier elements like silicon do not show that feature. Moreover, all nuclear species exhibit a comparable increase of the loss lengths and a corresponding shift to higher energies of the dominance region for CMB interactions.

Due to the changed energy loss lengths, the horizon for UHECRs is increased: for protons at all energies, for nuclei at the highest energies starting from $\sim A \times 10^9$ GeV. With such an increase the protons from sources at redshift 1 and energies $1 - 40$ EeV would propagate for several hundreds of megaparsecs more than under U(1), whereas protons at higher energies (where the photopion interactions prevail) would propagate for more than ten megaparsecs. However, as the redshift evolves to the present, the U(1) and SU(2) densities become the same and by distances of 20 Mpc the loss lengths differ by only 1.5 %. Thus, protons can propagate further away from sources beyond

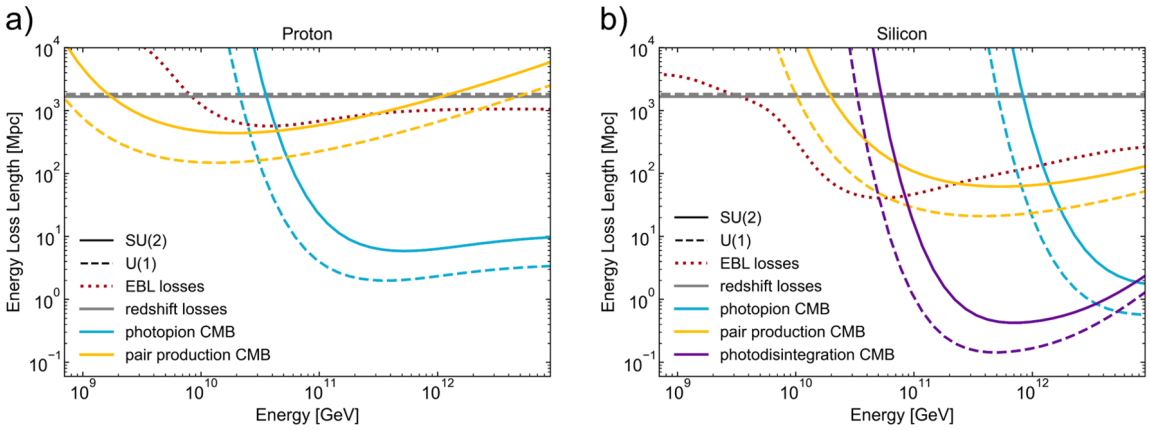

Figure 1: a) The propagation length of proton is given in Mpc dependent on the initial particle energy in GeV. The normal U(1) propagation length at redshift $z = 1$ is shown in dashed lines, the SU(2) induced $T(z)$ modification is shown in dot-dashed lines. b) The propagation length of silicon is given in Mpc dependent on the initial particle energy in GeV, also at redshift $z = 1$.

~200 Mpc in the SU(2) case. However, they lose their energy fully before reaching our galaxy. Nuclei experience a similar increase of horizon for the same reasons, however such increase is limited to energies above $\sim A \times 10^9$ GeV. For these energies, their propagation lengths are limited to a few tens of Mpc, and thus they experience less than 2 % increase of the loss lengths.

4. Propagation of UHECRs

In order to evaluate the impact of the modified $T(z)$-relation on the propagation of UHECRs, we start by using the best fit obtained by [15] to Auger data from 2017 [1] for a normal temperature redshift relation (ΛCDM). The spectral energy and composition changes using the modified $T(z)$ under $SU(2)_{CMB}$ are obtained to the same fit values for comparison. The propagation of the UHECRs was performed using PriNCe [15], which is an efficient code to integrate the transport equations for the evolution of cosmic rays at cosmological scales. It includes all the relevant interactions and allows for custom modifications, however, it does not account for the effect of magnetic fields. The propagation scenario considers a population of sources with a continuous distribution in redshift proportional to $(1 + z)^m$ with the source evolution parameter m obtained from the fit. The sources are homogeneous and eject a rigidity dependent spectral energy flux with the form

$$J_A(E) = \mathcal{J}_A \, f_{\text{cut}}(E, Z_A, R_{\text{max}}) \, (1 + z)^m \left(\frac{E}{E_0}\right)^{-\gamma}, \tag{8}$$

with five nuclear mass groups indicated by the index $_A$ (denoting the nuclear species ^{1}H, ^{4}He, ^{14}N, ^{28}Si, and ^{56}Fe). They share the same spectral index γ and the maximal rigidity $R_{\text{max}} = E_{\text{max}}/Z_A$. The cut-off of the injection spectra f_{cut} is defined as

$$f_{\text{cut}}(E) = \begin{cases} 1, & E < Z_A R_{\text{max}} \\ \exp\left(1 - E/(Z_A R_{\text{max}})\right), & E > Z_A R_{\text{max}}. \end{cases} \tag{9}$$

The $\mathcal{J}_A$ represent the flux of particles of species A emitted per unit of time, comoving volume, and energy. The elemental injection fractions f_A are defined as $f_A = \mathcal{J}_A / \Sigma_{A'} \mathcal{J}_{A'}$ at the reference energy E_0. The reference energy E_0 is set to $E_0 = 10^9$ GeV. Integrating over the injected fluxes J_A leads to the integral fraction of the energy density I_A, which are independent of the arbitrary choice of the reference energy E_0:

$$I_A = \frac{\int_{E_{\min}}^{\infty} J_A E \, dE}{\Sigma_{A'} \int_{E_{\min}}^{\infty} J_{A'} E \, dE} = \frac{\int_{E_{\min}}^{\infty} f_A \, f_{\text{cut}}(E, Z_A) \, E^{1-\gamma} dE}{\Sigma_{A'} \int_{E_{\min}}^{\infty} f_{A'} \, f_{\text{cut}}(E, Z_{A'}) \, E^{1-\gamma} dE}, \tag{10}$$

where $E_{\min} = 10^9$ GeV. For the sake of completeness, we will provide f_A and I_A. For $\text{SU(2)}_{\text{CMB}}$ the following cosmological parameters were used for the propagation: The Hubble parameter H_0= 74.24 $\text{km}\,\text{s}^{-1}\text{Mpc}^{-1}$, a dark energy fraction of $\Omega_\Lambda = 0.616$, and the local matter density $\Omega_{\text{m},0} = 0.384$, compare [13]. For U(1)_{CMB} (ΛCDM) the values from the Planck Collaboration were used [5, p. 15, Table 2], where $H_0 = 67.36$ $\text{km}\,\text{s}^{-1}\text{Mpc}^{-1}$, $\Omega_\Lambda = 0.6847$ and $\Omega_{\text{m},0} = 0.3153$ (TT,TE,EE+lowE+lensing). The best fit parameters of [15] can be seen in Table 1 and Fig. 2 shows a comparison of the fluxes obtained with the same parameters by employing the $T(z)$ relation for SU(2) (solid lines) vs. ΛCDM (dashed lines).

EBL	Gilmore et al.	Element	f_A %	I_A %
models	Talys & Sibyll 2.3c	H	0.0	0.0
redshifts	1 - 0	He	82.0	9.91
γ	-0.8	Ni	17.3	69.99
$R_{\max}$	1.6×10^9 GV	Si	0.6	16.91
m	4.2	Fe	0.02	3.19

Table 1: Best fit parameters from [15], Table 3.

The resulting total flux for SU(2) is virtually unchanged for energies above 6×10^9 GeV while the fluxes for individual nuclear groups present slightly more pronounced peaks. This effect is a consequence of the modest increase in the horizons. At the same time, the reduction in the pair production losses produces sharper peaks because the effect of energy redistribution corresponding to the U(1) cases are less prominent for SU(2). For protons at the lowest energies, the differences are much more pronounced due to the change in pair production rates as the energies approach 10^9 GeV from above.

The expected cosmogenic neutrino fluxes are shown in Fig. 2 b) for the modified temperature redshift relation under $\text{SU(2)}_{\text{CMB}}$. The neutrino fluxes for $\text{SU(2)}_{\text{CMB}}$ peak at slightly higher energies and are slightly increased. The former feature is a consequence of the delayed increase of the CMB densities in $\text{SU(2)}_{\text{CMB}}$ compared to U(1), which shifts the photopion production towards lower redshifts. Indeed, the redshift scaling of the photopion interactions implies that a delayed production occurs with lower-energy counterpart photons for which protons with larger boosts are needed to reach the photopion thresholds and hence explaining the larger energies of the resulting neutrinos from pion decay. The slightly increased flux of neutrinos results from the increased horizons of the $\text{SU(2)}_{\text{CMB}}$.

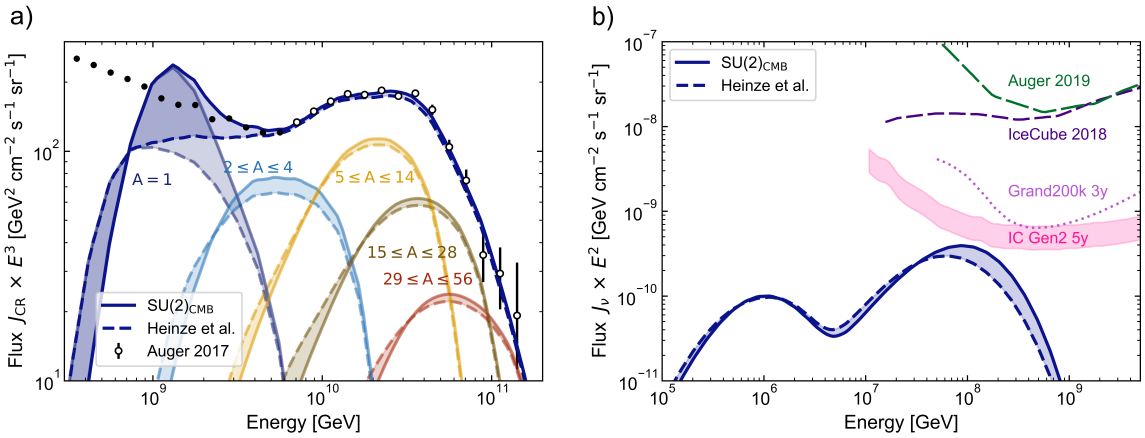

Figure 2: a) Spectral fit to the 2017 Auger spectral flux data [1] from the best fit parameters in [15], see Tab. 1. The total flux of the normal U(1) temperature redshift relation is shown in a navy blue dashed line. The total cosmic ray flux with an SU(2) temperature redshift relation is shown with a navy blue solid line. The χ^2 used in this fit only consider data points including the ankle region (white dots), compare [15]. b) The cosmogenic neutrino flux obtained from the best fit parameters as used in a). $SU(2)_{CMB}$ is shown in navy blue, normal ΛCDM with the corresponding cosmological parameters and U(1) photon propagation is shown in a navy blue dashed line. The pink shaded area represents the projected sensitivity for the IceCube Gen2 radio upgrade after 5 years of observation, compare Fig. 5 in [4]. The lavender doted line indicates the expected sensitivity for Grand200k after 3 years [6]. The dark purple dashed line shows 90% CL limits from the IceCube Collaboration (2018) [3], and the green dashes line represents the 90% CL limit from the Pierre Auger Collaboration (2019) [2].

In addition to the cosmogenic neutrinos, the photopion production in the CMB also generates γ-rays and due to the increased horizon in the case of a $SU(2)_{CMB}$, the resulting flux would have been slightly enhanced compared to the $U(1)_{CMB}$, if the produced gamma-ray had not suffered $\gamma\gamma$-pair production. However, since $\gamma\gamma$-pair production and inverse Compton scattering yield an electromagnetic cascade, which is strongly affected by the impact of the EBL, in particular at γ-ray energies $\lesssim 100\,\mathrm{TeV}$, we expect no significant difference in the cosmogenic γ-ray flux between the $SU(2)_{CMB}$ and the $U(1)_{CMB}$.

5. Summary and Outlook

In this work, we examined the impact of a non-linear modification of the CMB temperature redshift relation $T(z)$ on the fit to ultra-high energy cosmic rays. This changed temperature redshift relation is motivated by assuming an SU(2) rather than a U(1) gauge group to describe CMB photons. While the temperature redshift relation is locally ($z = 0$) the same as in ΛCDM, the spectral CMB density increases non-linearly slower for small redshifts ($z \lessapprox 4$) under $SU(2)_{CMB}$, and then linear with a scaling factor of $1/4^{1/3} \approx 0.63$ in comparison to the normal $T(z)$ under ΛCDM.

The reduction of the CMB densities is found to affect significantly the interaction lengths of UHECRs with CMB photons in the redshift range of relevance for UHECR propagation, resulting in extended horizons for protons and UHECR nuclei. However, the increase in interaction lengths

does have only a modest effect on the observed UHECR flux due to interactions with the EBL, which then become dominant for the energies of relevance. Hence, a comparison to an existing fit of UHECRs yields a similar flux of UHECRs nuclei, but differs considerably for protons where a pronounced bump appears below the ankle in the $SU(2)_{CMB}$ scenario. This proton bump may add another tool to discriminate potential UHECR source classes. With future constraints on the UHECR source classes, the abundance of protons below the ankle may be a useful probe for the temperature redshift relation $T(z)$ of the CMB in the future.

6. Data availability

The authors welcome requests to collaborate, and will share the modifications of Jonas Heinze's original program PriNCe as used in this study accordingly.

7. Acknowledgements

JM acknowledges insightful discussions with Dr. Ralf Hofmann and Professor Wolfgang Rhode. This work is supported by the Vector Foundation under grant number P2021-0102 and by the SFB 1491 (Project A3). LM's work is supported by the DFG under grant number 445990517 (KA 710).

References

[1] Aab A., et al., 2017, J. Cosmol. Astropart. Phys., 04, 038
[2] Aab A., et al., 2019, J. Cosmol. Astropart. Phys., 10, 022
[3] Aartsen M. G., et al., 2018, Phys. Rev. D, 98, 062003
[4] Aartsen M. G., et al., 2019, Neutrino astronomy with the next generation IceCube Neutrino Observatory (arXiv:1911.02561)
[5] Aghanim N., et al., 2020, Astron. Astrophys., 641, A6
[6] Álvarez-Muñiz J., et al., 2020, Sci. China Phys. Mech. Astron., 63, 219501
[7] Berezinskii V. S., Bulanov S. V., Dogiel V. A., Ptuskin V. S., 1990, Astrophysics of cosmic rays
[8] Caputo A., Regis M., Taoso M., Witte S. J., 2019, JCAP, 03, 027
[9] Dowell J., Taylor G. B., 2018, Astrophys. J. Lett., 858, L9
[10] Fixsen D. J., et al., 2011, Astrophys. J., 734, 5
[11] Hahn S., Hofmann R., 2017, Mon. Not. Roy. Astron. Soc., 469, 1233
[12] Hahn S., Hofmann R., 2018, Mod. Phys. Lett. A, 2016, 1850029
[13] Hahn S., Hofmann R., Kramer D., 2019, Mon. Not. Roy. Astron. Soc., 482, 4290
[14] Harrington B. J., Shepard H. K., 1978, Phys. Rev. D, 17, 2122
[15] Heinze J., Fedynitch A., Boncioli D., Winter W., 2019, Astrophys. J., 873, 88
[16] Hofmann R., 2009, Annalen Phys. (Berlin), 18, 634
[17] Hofmann R., 2016, The thermodynamics of quantum Yang-Mills theory: Theory and applications, 2nd edition. World Scientific
[18] Hofmann R., Meinert J., 2023, Frequency-redshift relation of the Cosmic Microwave Background (arXiv:2303.16744)
[19] Mather J. C., Fixsen D. J., Shafer R. A., Mosier C., Wilkinson D. T., 1999, Astrophys. J., 512, 511
[20] Riechers D. A., Weiss A., Walter F., Carilli C. L., Cox P., Decarli R., Neri R., 2022, Nature, 602, 58
[21] Seiffert M., et al., 2011, The Astrophysical Journal, 734, 6
[22] Tipler F. J., Piasecki D. W., 2018, Using UHE Cosmic Rays to Probe the CBR and Test Standard Model Particle Physics (arXiv:1809.08492)
[23] Tompkins S. A., Driver S. P., Robotham A. S. G., Windhorst R. A., Lagos C. d. P., Vernstrom T., Hopkins A. M., 2023, Mon. Not. Roy. Astron. Soc, 521, 332